CHARACTERIZATION OF OLD CONCRETE FOR NEW USE: GRID NANOINDENTATION AND SCANNING ELECTRON MICROSCOPY

Zdeněk PROŠEK, Pavel TESÁREK, Vladimír HRBEK

Czech Technical University in Prague, Faculty of Civil Engineering,
Prague, Czech Republic, EU,
zdenek.prosek@fsv.cvut.cz, pavel.tesarek@fsv.cvut.cz, vladimir.hrbek@fsv.cvut.cz

Abstract

Concrete waste after further processing can be used in the form of a micronized powder in which the non-hydrated portions are reactivated. For this purpose, nanoindentation and scanning electron microscopy with X-ray spectroscopy (SEM-EDS) are combined to determine properties of the concrete sample. The approximate composition of old concrete is calculated from SEM BSE image analysis. The nanoindentation technique over two main material levels enabled evaluation of the indentation modulus of these phases due to the spectral deconvolution of measured data. All these techniques serve for determining the activity of old concrete and characterization shape and textures of activation micronized old concrete powder.

Keywords: Old concrete, nanoindentation, SEM analysis, micronized powder

1. INTRODUCTION

Construction creates the high amount of waste from all sectors. Construction waste is almost 33 % of the 2.5 billion tons of waste generated in the EU [1]. The old concrete is taken to the recycling line. Materials from recycling facilities are most often used as coarse aggregates in new concrete, but only coarse fractions are processed [2]. In the case of a very fine fraction (grain size below 1 mm), there is still no ideal solution to allow its use on a broader scale. Several possible ways of application of this material are examined in cement composites for example as thermally activated binder replacement [3], as mixtures for cement production [4] or as a part of geopolymers based binders [5]. Due to high demands on energy consumption and CO2 production the most sophisticated and environmentally friendly method is when the very fine fraction of recycled concrete is used in its raw form.

For this reason, the paper deals with the possibility of mechanical activation of concrete recyclate with high-speed milling. Mechanical activation of the old concrete occurs when hydrated cement paste is milled, and this reveals still non-hydrated grains of clinker. The amount of non-hydrated clinker is directly dependent on the type of cement and the age of the old concrete. In general, the amount of non-hydrated clinker in the cement matrix can be estimated between 10 to 20 % [6]. Up to 20 % of old concrete can be reactivated and can form binder in the future concrete and the remaining amount will be inert and can form a filler. Micronized milling process can reduce not only the amount of cement but also the amount of natural filler in future concrete [7]. Since up to approximately from 80 to 90 % of the total volume of old concrete consists of inert particles, inert particles characteristics significantly affect the performance of use of old concrete in a new production. Shape and texture of fine inert particles have the most significant impact on the resulting properties of fresh and hardened concrete. The inert particles not only make concrete economical by occupying more volume but also impart volume stability and increase durability [8]. Shape and texture of particles have a significant effect on the performance of fresh concrete. Concrete mixture with well-shaped, rounded, and smooth particles require less amount of cement paste on the excellent workability of fresh mixtures than mixtures with flat, elongated, angular, and rough particles. As a result, well-shaped particles will have less durability caused by the paste such as heat generation, porosity, and drying shrinkage [9].

2. EXPERIMENTAL

For the experiment on mechanical activation of old concrete was used recycled concrete made of concrete railway sleepers. The used old concrete is a material that has already undergone a recycling process (steel reinforcement was removed, and the concrete was pre-crushed). For our purposes, we used a fraction of 0-4mm that does not have a practical use for reuse in new concrete. Concrete sleepers were PB2 and SB8, which was 50 years old.

In the first step, the experiment examined concrete fractions of 0-4 mm. For this purpose, a combination of methods: nanoindentation for determination of micromechanical properties and electron microscopy with EDS detector was used. In the second step, fractions 0-4 were mechanically activated using the micro-milled process. The fine milling of the material was delivered by the company Lavaris Ltd. (procedure protected by patents) using the high-speed milling technique. Subsequently, the micronized concrete powder was subjected to image analysis using an electron microscope. The image analysis provided information on the shape, activation, and suitability of micronized concrete powder for further use.

2.1. Sample preparation

For the investigation, the sample of old concrete (fraction 0-4 mm) and micronized concrete powder were embedded in epoxy resin. Parts of specimens were cut (approx. thickness 15 mm), and silica-carbon papers and diamond suspensions were used for grinding and polishing of the specimen surface. Polished sections were prepared on a Tegramin from Struers. The samples were polished in multiple steps to achieve the best surface quality of the samples. This technique ensured adequate surface roughness of the sample for both indentation and SEM investigation. The coordination mark was inscribed on the polished surface, serving as the origin for further orientation. The mark enabled the positioning of both investigation techniques in the same area of the sample.

2.2. Nanoindentation

The technique of nano-indentation (Ti 750 series, Hysitron Inc.) was applied on the specimen to evaluate elastic mechanical properties (Young's modulus and hardness) of the material. For the purpose of this study, the displacement driven load function with "loading" and "unloading" segments lasting 5 seconds each with an in-between 60 seconds of "holding" time segment was adopted. The maximum prescribed indentation depth was selected 150 nm. The measurement setting meets the grid-indentation specifications of the heterogeneous composite with further application of spectral deconvolution on obtained data [10-14].

The measurement was performed on two crucial levels of the composite (cementitious matrix and aggregate-matrix inter-phase zone) to achieve efficient investigation of each material phase. The first level grid (located in the matrix) was designed for detailed evaluation of phases present in cement paste. The grid consisted of 25 by 25 indents separated by 2 μm (covering area approx. 17.26 %). Grid applied on inter-phase zone location was constructed of 21 by 21 indents in pattern with 5 μm spacing (covering 2.81 % of total area of the grid).

2.3. Electron microscopy

The investigation of the samples consisted of two main techniques, scanning electron microscopy combined with Energy Spectrometer (SEM-EDS) and backscattered electron images with image analysis (SEM BSE-IA). As a result, with nanoindentation, a combination of micromechanical properties, phases chemical composition and material structure enabled the proper description of the material.

The scanning electron microscopy (SEM) investigation was performed on FEG SEM Merlin ZEISS on polished specimens coated with a thin layer of carbon necessary to ensure proper conductivity of the surface. The FEG SEM Merlin ZEISS scanning electron microscope is located in the Laboratory of Electron Microscopy and Microanalysis at the University Center of Energy Efficient Buildings. Qualitative and quantitative analysis of the

chemical composition of the samples was performed using an X-ray microanalysis, namely an Energy Spectrometer (EDS) by Oxford Instruments. The point ID method was used in the first step, where only selected areas (areas near indents) were tested. Five microanalyses were performed to determine the weight and atomic representation of individual elements in percent for each phase. The resulting phase was calculated by using stoichiometry. The working distance of the electron microscope was set to 8.5 mm, the accelerating voltage was set to 15 kV, and the current was set to 1 nA. This set up provides a good signal.

Backscattered electron images (SEM-BSE) was performed on FEG SEM Merlin ZEISS with same set up as in the previous case. SEM-BSE has energy comparable to that of the primary electron beam. They come out of greater depth (tens of millimeters in diameter) and thus provide information on local material changes. The information is a material contrast (each phase has its shade of gray). Their resolution is 50-200 nm, which is sufficient in our case. When combining SEM-BSE and image analysis (IA), we get not only the phase contrast but also the percentage representation of the individual phases and the character of the individual grains. The calculation of phase volumetric representations in the viewed field of each phase was performed by Phase Analysis 1.1 (software). Determination of structure and character of individual particles was performed by ImageJ-Analyze particles (software). SEM-BSE IA was made from 64 images at 1k× magnification and 1024×768 px resolution. Such a number of images covers an area of 2.05 mm x 2.05 mm, i.e., 4.2 mm^2.

Structure and character of individual particles were determined by a set of parameters describing the shape of the particle. These shape descriptors were circularity, aspect ratio, roundness, and ferret angle. The circularity (Circ.) describes how particles similar to a circle with a value of 1.0 indicating a perfect circle and value of near to 0.0 indicates an increasingly elongated shape. The value of circularity is calculated by equation (1):

$$Circ. = 4 \cdot \pi \frac{A}{P^2} \tag{1}$$

where:

Circ. - the circularity (-)
A - the area of grain (μm^2)
P - the perimeter (The length of the outside boundary of the grain) (μm).

The aspect ratio (2) is defined as:

$$AR = \frac{MA}{MI} \tag{2}$$

where:

AR. - the aspect ratio of the particle's fitted ellipses (-)
MA - the major axis (the length of the longest axis best fitting ellipse to grain) (μm)
MI - the minor axis (the length of the shortest axis best fitting ellipse to grain) (μm).

The roundness (3) is also a useful parameter for describing the similarity degree of a particle to a circle. Unlike circularity, roundness calculates with rough edges. The roundness is a shape factor that has a maximum value of 1 for a circle and lower values for shapes having a higher ratio of perimeter to area, longer or thinner shapes, or objects having rough edges. For the image analysis used in this experiment, Roundness is defined as:

$$Round. = 4 \frac{A}{\pi \cdot MA^2} \tag{3}$$

where:

Round. - the roundness (-)
A - the area of grain (μm^2)
MA - the major axis (the length of the longest axis best fitting ellipse to grain) (μm).

Feret angle is the angle between the longest side of the grain and the shortest side of the grain.

3. RESULTS AND DISCUSSION

Figure 1 shows SEM images in BSE mode of old concrete and micronized old concrete with the same magnification. BSE image shows white for non-hydrated clinker, light gray for the cement matrix, gray for quartz (aggregate) and dark gray or black for pore, crack or epoxy resin. Also, there are three other phases in the cement matrix, which have different micromechanical properties, namely low-density C-S-H gel, high-density C-S-H gel, and portlandite. Micromechanical properties namely reduced the modulus of individual phases were 19.2 ± 3.5 GPa for low-density C-S-H gel, 39.8 ± 6.0 GPa for high-density C-S-H gel, 58.6 ± 6.3 GPa for portlandite, 79.8 ± 3.1 GPa for quartz and 118.4 ± 16.9 GPa for non-hydrated clinker. **Table 1** shows the result of SEM BSE IA. The results show approximately 5.6 % clinker in old concrete. Micronized old concrete had 2.5 % of clinker, but if percentage value was calculated without epoxy resin, the amount was still the same as for old concrete, namely 5.1 %. This fact, however, does not apply in the case of a cement matrix, where the quantity has been reduced by up to 20 %. This fact was most likely due to the low mechanical properties and milling of the cement matrix into dust particles that were not captured by the filter. Also, it can be seen in **Figure 1** that mechanical re-activation of the already hydrated clinker has occurred partly by their uncover.

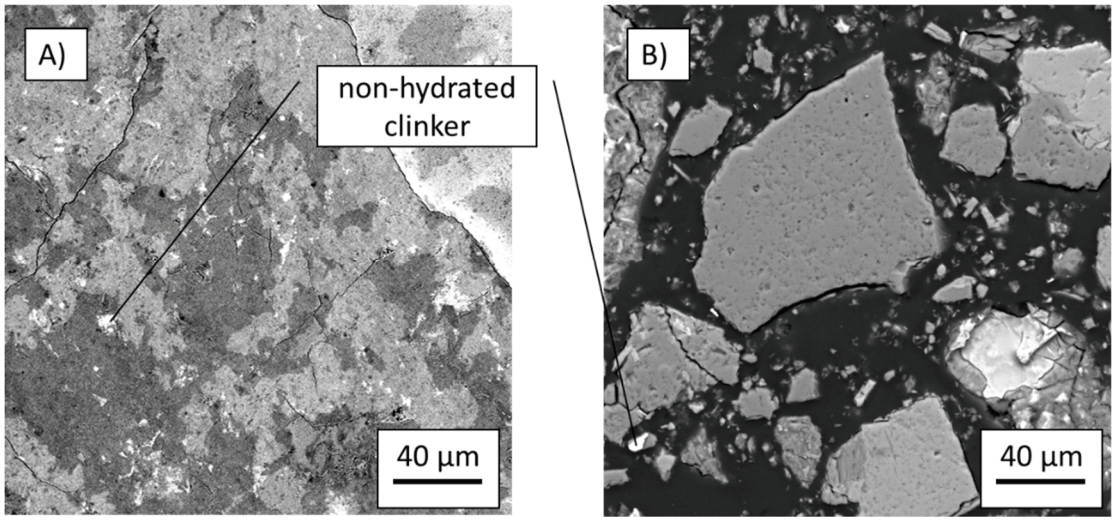

Figure 1 BSE images of microstructure, magnification 1k× a) old concrete, b) micronized old concrete

Table 1 Results of phase volumetric representations in viewed field

Material	Clinker (%)	Cement matrix (%)	Quartz (%)	Pore / Epoxy (%)
Old Concrete	5.6 ± 0.5	48.1 ± 2.1	45.6 ± 1.5	0.7 ± 0.1
Micronized Old Concrete	2.5 ± 0.2	6.6 ± 0.9	41.8 ± 3.5	49.1 ± 3.5

Figure 2 shows a grain characterization procedure where the individual grains are replaced by a fitting ellipse describing their shape. The individual phases were not separated by the micro-milled process so that the shape characterization was performed on all grains. Results in the form of shape descriptors are shown in **Table 2**. During the analysis, more than 91,000 grains were examined. Value of circularity was equal to 0.73. This value determines that the grains are slightly elliptical than the circular shape. The value of roundness was equal to 0.57, so although grains are elliptical, the perimeter is very uneven due to rough edges. Aspect ratio was equal to 2.03, so grains had a slightly elongated shape. The Feret angle was 96.3°, the value is very close to 90°, and therefore characterization of shape grain can be used by fitting ellipse technique.

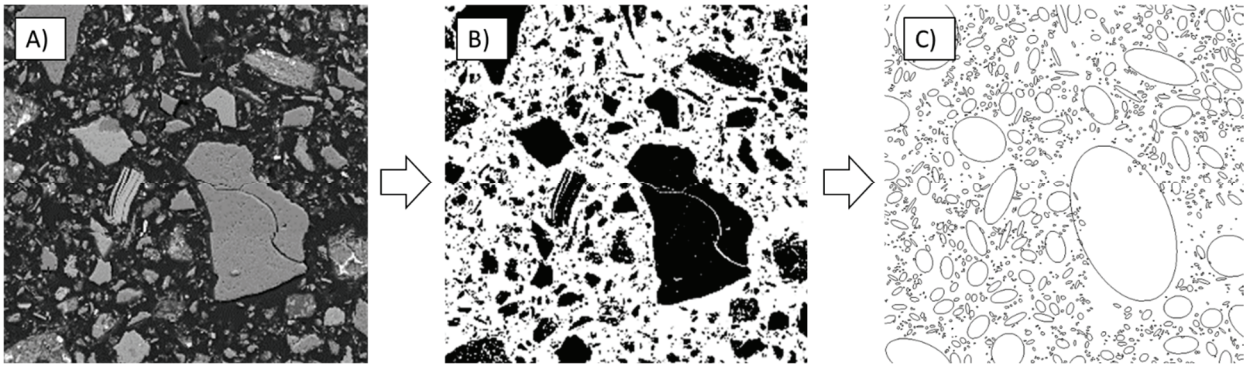

Figure 2 Image analysis of BSE images: A) BSE image, B) marking grains, C) fitting an ellipse to grain

Table 2 Summary of a parameter describing the shape of grains

Material	Count (pc.)	Circularity (-)	Roundness (-)	Feret Angle (°)	Aspect ratio (-)
Micronized Old Concrete	91115	0.73 ± 0.13	0.57 ± 0.11	96.3 ± 12.5	2.03 ± 0.3

4. CONCLUSION

This work deals with the use of high-speed milling technique for recycling of old concrete and the direct characterization of the old concrete and micronized old concrete. Two different experimental methods were used for this purpose, and the results show that:

- Tested old concrete contained approximately 5 % of non-hydrated clinkers that were uncovered by the high-speed grinding process and reactivated;
- SEM-BSE images showed the grains of non-hydrated clinker were uncovered only partially;
- The high-speed milling process had a negative effect on the amount of old cement matrix, where the amount was reduced by 20 % due to low mechanical properties;
- Grains of micronized old concrete has an elongated ellipse shape with rough edges.

In the future, the work will focus on other different types of concrete waste, such as monolithic structures, concretes for supporting structures and concretes for transport infrastructure. The concrete will have different compositions depending on their properties as well as varying amounts of non-hydrated clinker and the strength of the individual phases.

ACKNOWLEDGEMENTS

This was financially supported by the Czech Science Foundation research projects 17-06771S and by the Czech Technical University in Prague project SGS16/201/OHK1/3T/11.

REFERENCES

[1] Waste statistics. In: EUROSTAT. Date: 04-04-17 [update]. [viewed 2018-09-27]. Available from https://ec.europa.eu.

[2] XIAO, Jianzhuang, LI, Wengui, FAN, Yuhui, HUANG, Xiao. An overview of study on recycled aggregate concrete in China (1996-2011), *Construction and Building Materials.* 2012. vol 31, pp. 364-383.

[3] SHUI, Zhonghe, XUAN, Dongxing, WAN, Huiwen, CAO, Beibei. Rehydration reactivity of recycled mortar from concrete waste experienced to thermal treatment, *Construction and Building Materials*. 2008. vol. 22, pp. 1723-1729.

[4] SCHOON, Joris, HEYDEN, Luc Van der, ELOY, Pierre, GAIGNEUX, Eric M., BUYSSER, Klaartje De, DRIESSCHE, Isabel Van, BELIE, Nele De. Waste fibrecement: An interesting alternative raw material for a sustainable Portland clinker production, *Construction and Building Materials,* 2012. vol. 36, pp. 391-403.

[5] AHMARI, Saeed, REN, Xin, TOUFIGH, Vahab, ZHANG Lianyang. Production of geopolymeric binder from blended waste concrete powder and fly ash, *Construction and Building Materials.* 2012. vol. 35, pp. 718-729.

[6] TOPIČ, Jaroslav, PROŠEK, Zdeněk, FLÁDR, Josef, TESÁREK, Pavel. Vliv jemnosti recyklované betonové moučky na vývin hydratačního tepla a vliv jejího množství na mechanickofyzikální vlastnosti cementové pasty, *Wate Forum*. 2018. vol. 2, pp. 268-274.

[7] PROŠEK, Zdeněk, TOPIČ, Jaroslav, ĎUREJE, Jakub, TREJBAL, Jan. Srovnání vlivu mikromletého betonu a mramorové moučky na mechanické vlastnosti cementových past, *Waste Forum.* 2018. vol. 2, pp. 262 - 267.

[8] KWAN, Albert KH; MORA, C. F.; CHAN, H. C. Particle shape analysis of coarse aggregate using digital image processing. *Cement and Concrete Research*. 1999. vol. 29. no. 9, pp. 1403-1410.

[9] ERDOGAN, S. T., et al. Three-dimensional shape analysis of coarse aggregates: New techniques for and preliminary results on several different coarse aggregates and reference rocks. *Cement and Concrete Research*, 2006. vol. 36, no. 9, pp. 1619-1627.

[10] OLIVER, Warren C., PHARR, George M. An improved technique for determining hardness and elastic modulus using load and displacement sensing indentation experiments. *Journal of materials research*. 1992. vol. 7, no. 6, pp. 1564-1583.

[11] PHARR, G. M., BOLSHAKOV, A. Understanding nanoindentation unloading curves. *Journal of Materials Research*. 2002. vol. 17, no. 10, pp. 2660-2671.

[12] OLIVER, Warren C., PHARR, Georges M. Measurement of hardness and elastic modulus by instrumented indentation: Advances in understanding and refinements to methodology. Journal of materials research. 2004. vol. 19, no.1, pp. 3-20.

[13] CONSTANTINIDES, Georgios, et al. Grid indentation analysis of composite microstructure and mechanics: Principles and validation. *Materials Science and Engineering: A*. 2006. vol. 430, no.1-2, pp. 189-202.

[14] ULM, Franz-Josef, et al. Statistical indentation techniques for hydrated nanocomposites: concrete, bone, and shale. *Journal of the American Ceramic Society*. 2007. vol. 90, no. 9, pp. 2677-2692.